

CONSTRAINTS ON NEUTRON-STAR RADII FROM LABORATORY EXPERIMENTS*

SAKIB RAHMAN

PREX-2/CREX Collaboration

University of Manitoba, Canada

*Received 16 December 2022, accepted 2 January 2023,
published online 22 March 2023*

High-precision measurements of asymmetry in parity-violating electron–nuclei scattering experiments enhance our understanding of the structure of nuclei and neutron stars. PREX-2 and CREX (Lead/Calcium Radius Experiments) are two recent experiments conducted at JLab in Newport News, Virginia, USA, by elastically scattering an electron beam with rapidly flipping helicity from ^{208}Pb and ^{48}Ca targets, respectively. PREX-2 measured an asymmetry $A_{\text{PV}}^{208} = 550 \pm 16$ [stat.] ± 8 [sys.] ppb at kinematics with mean $Q^2 \sim 0.00616$ GeV 2 . Together with the predecessor PREX-1, it constrained the ^{208}Pb neutron skin to $R_{\text{skin}}^{208} = 0.283 \pm 0.071$ fm. The combined constraint on nuclear DFT models from PREX and the NICER telescope neutron-star radii measurements is in ~ 1 standard deviation tension with the constraint from the LIGO tidal deformability measurements. CREX was conducted at kinematics with mean $Q^2 \sim 0.0297$ GeV 2 , resulting in an asymmetry $A_{\text{PV}}^{48} = 2668 \pm 106$ [stat.] ± 40 [sys.] ppb and the ^{48}Ca neutron skin $R_{\text{skin}}^{48} = 0.121 \pm 0.026$ [exp.] ± 0.024 [model] fm respectively. The CREX result contrasts the PREX result by predicting a thinner neutron skin for medium-mass nuclei compared to heavy nuclei. Understanding these anomalies with further studies is necessary to pin down the density-dependence of nuclear symmetry energy and constrain neutron-star radii accurately.

DOI:10.5506/APhysPolBSupp.16.4-A7

1. Introduction

The weak interaction is the only known fundamental interaction that violates parity. In a parity-violating electron scattering experiment, a polarized electron beam with rapidly flipping spin is scattered from stationary targets such as nuclei. The alignment between the spin (\mathbf{s}) and momentum (\mathbf{p}) of

* Presented at the Zakopane Conference on Nuclear Physics, *Extremes of the Nuclear Landscape*, Zakopane, Poland, 28 August–4 September, 2022.

the beam electrons determines the helicity. For relativistic electrons, helicity can be correlated with handedness [Figure 1]. The relative difference between the interaction cross sections of scattered electrons in opposite helicity states is termed as the parity-violating asymmetry (A_{PV}). Thus,

$$A_{\text{PV}} = \frac{\sigma_{\text{R}} - \sigma_{\text{L}}}{\sigma_{\text{R}} + \sigma_{\text{L}}}, \quad (1)$$

where σ_{R} and σ_{L} are the scattering cross sections for right-handed and left-handed electrons respectively [1, 2].

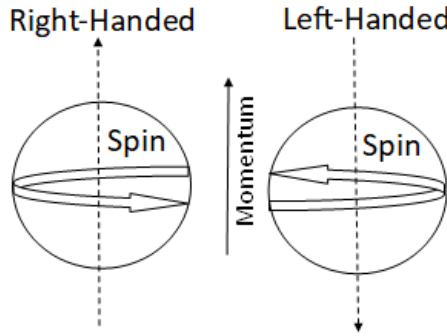


Fig. 1. Helicity. The figure is reused [4].

PREX-2 and CREX measured the neutron skins of the ^{208}Pb and ^{48}Ca nuclei by measuring the parity-violating asymmetry in polarized electron–nuclei elastic scattering. In any neutron-rich nucleus, the neutron distribution is spread farther out than the proton distribution due to the nuclear symmetry pressure acting against the surface tension. Thus, a neutron skin is formed [3]. The weak charge distribution closely approximates the neutron distribution. In addition, the relationship between the parity-violating asymmetry and the weak charge distribution can be expressed by the following equation:

$$A_{\text{PV}} \approx \frac{G_{\text{F}} Q^2 |Q_{\text{W}}| F_{\text{W}}(Q^2)}{4\sqrt{2}\pi\alpha Z F_{\text{ch}}(Q^2)}, \quad (2)$$

where A_{PV} is the parity-violating asymmetry, G_{F} is the Fermi coupling constant, Q_{W} is the weak charge of the nucleus, Q is the four-momentum transfer magnitude, and $F_{\text{W}}/F_{\text{ch}}$ is the weak/electric form factor, *i.e.*, the Fourier transform of the weak/electric charge distribution [1, 2].

The experimentally measured asymmetry cannot be directly compared with theory without considering the acceptance function ($\epsilon(\theta)$), the normalized distribution of elastic scattering angles intercepting the main detectors, defined by the experimental setup. The average asymmetry ($\langle A \rangle$) to compare against can be extracted from the theoretically modelled asymmetry

function ($A(\theta)$) taking into account the differential scattering cross section $\frac{d\sigma}{d\Omega}$ and the acceptance function ($\epsilon(\theta)$) as follows [1, 2]:

$$\langle A \rangle = \frac{\int d\theta \sin(\theta) A(\theta) \frac{d\sigma}{d\Omega} \epsilon(\theta)}{\int d\theta \sin(\theta) \frac{d\sigma}{d\Omega} \epsilon(\theta)}. \quad (3)$$

In the PREX-2/CREX analysis, a two-parameter Fermi function was fitted to the theoretical weak-charge densities ($\rho_W(r)$) from a wide range of non-relativistic and relativistic density functional models. The Fermi function was used to calculate the model asymmetry as a function of scattering angle which was then averaged over the acceptance using equation (3). Similarly, the weak charge form factor $F_W(Q^2)$ can be calculated at the experimental kinematics using the Fermi function [5]. In the limit $Q^2 \rightarrow 0$,

$$F_W(Q^2) - F_{\text{ch}}(Q^2) = \frac{Q^2}{6} (R_W^2 - R_{\text{ch}}^2), \quad (4)$$

where R_W is the R.M.S. radius of $\rho_W(r)$ and R_{ch} is the charge radius [2]. Since the kinematics for CREX did not satisfy this criterion, there is an additional model dependence in the extraction of the weak skin $R_W - R_{\text{ch}}$ and, consequently, the neutron skin $R_n - R_p$ in the case of CREX. The model correlations among the predicted form-factor differences, weak skins, neutron skins, and asymmetries can be used in coordination with the measured asymmetry to constrain the above quantities. Thus, an accurate measurement of the asymmetry guarantees a relatively model-independent and theoretically clean mode of constraining those values compared to experiments that use strong interaction probes [1, 2].

The thickness of neutron skins of heavy nuclei and the radii of neutron stars are both driven by the nuclear symmetry pressure at their respective densities. The symmetry pressure near nuclear saturation density is

$$P(\rho_0) \approx \frac{1}{3} L \rho_0, \quad (5)$$

where L is the slope of the symmetry energy with respect to density and ρ_0 is the nuclear saturation density [6]. ρ_0 is closely approximated by the interior baryon density in heavy nuclei. The predicted values of L from various models show a strong correlation with the predicted neutron skins ($R_n - R_p$). Thus, a precise constraint on L and the size of neutron-stars can be derived from the constraint on neutron-skin thickness.

2. The PREX-2 and CREX experiments

The PREX-2 and CREX experiments were both conducted at the Continuous Electron Beam Accelerator Facility (CEBAF) of the Thomas Jefferson National Laboratory (JLab) in Newport News, Virginia, USA. As

shown in figure 2, the polarized electron beam is produced in the injector. The injector features a Rubidium Titanyl Phosphate (RTP) Pockels cell which changes the polarization of a 780–850 nm laser beam from linear to circular. The handedness of the laser beam changes at regular intervals based on the pseudo-random input voltage pattern of the Pockels cell. The laser beam is then incident on a GaAs photocathode to produce the polarized electron beam with rapidly flipping helicity. There is an insertable half wave plate (IHW) in the injector region and a double Wien magnet assembly just downstream of the injector for slow helicity reversals. The polarized electron beam is accelerated by 1.1 GeV for each pass through the linear accelerators. The accelerator beamline features polarimeters and sensors that help to monitor beam quality from where the beam exits the injector to the experimental hall A where the PREX-2/CREX apparatus was set up. The highly polarized and intense beam, accompanied by precision beam control and monitoring capabilities, made JLab an attractive location to conduct PREX-2/CREX.

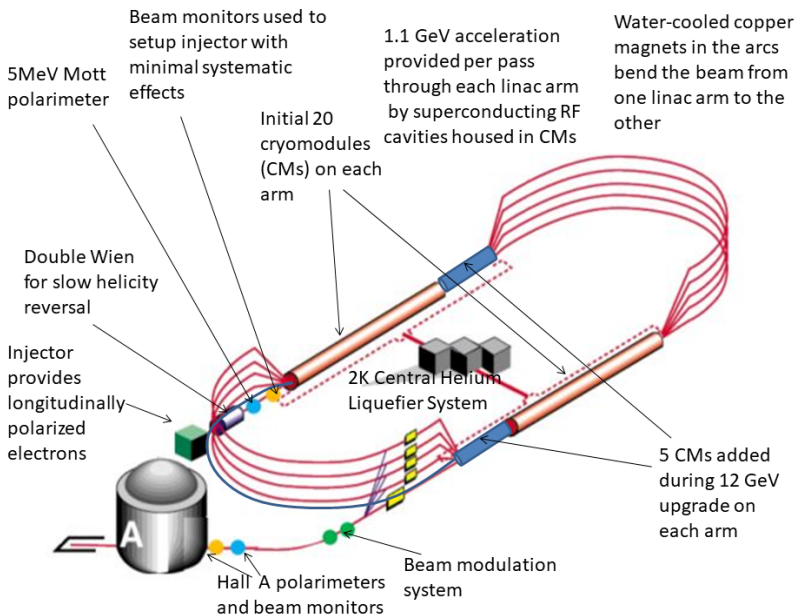


Fig. 2. Continuous Electron Beam Accelerator Facility. The figure is reused after modification with permission from the American Institute of Physics [7].

As shown in the scheme in figure 3, the PREX-2/CREX experimental setup can be divided into 3 distinct regions: the target chamber, the spectrometer magnets, and the detector huts. The aluminium target chamber housed two target ladders that were used for optics calibration and physics

measurement respectively. The physics ladder was cryogenically cooled and contained the main target samples. The electron beam was rastered in a $\sim 4\text{--}5\text{ mm}^2$ rectangular or square pattern to avoid damaging the target. The scattered electrons emerging at ~ 5 degree scattering angle were bent by a septum magnet to ~ 12.5 degrees into the acceptance-defining collimators at the entrance to the two High-Resolution Spectrometers (HRS) in the hall. Each HRS features 3 quadrupole magnets and 1 dipole magnet to provide radial and azimuthal focusing along the path to the detectors. The elastically scattered electrons were focused onto identical Cerenkov detectors with quartz tiles of $16 \times 3.5 \times 0.5\text{ cm}^3$ dimension on each arm of the HRS. The detectors were coupled with photo-multiplier tubes and had their longest sides oriented along the dispersive direction. The detector huts also featured vertical drift chambers and scintillators that were used occasionally for optics alignment, and auxiliary Cerenkov detectors that were used for transverse asymmetry measurements.

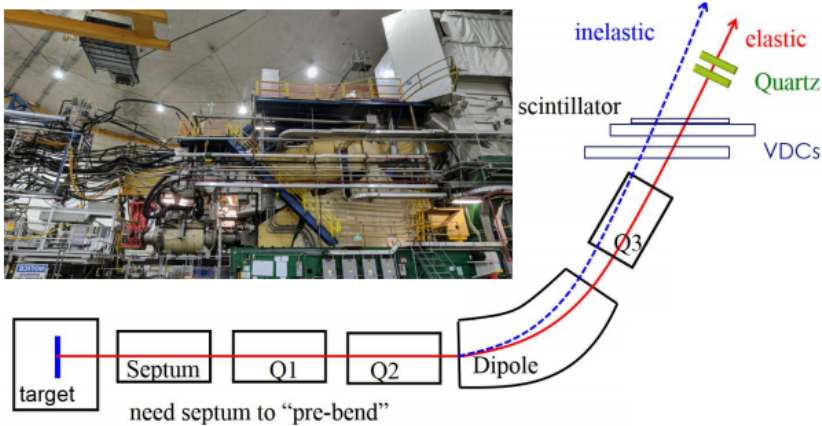


Fig. 3. Scheme of PREX/CREX apparatus. The figure is reused with permission from the author [8].

Fluctuation in helicity-correlated beam properties can lead to false asymmetries. Active feedback was used to control integrated beam charge asymmetry. Detector sensitivities were calculated with respect to forced modulation of the beam using air-core magnets and an RF cavity in the beamline. They were also checked with respect to the natural beam motion. The helicity-correlated asymmetries due to position and energy fluctuations were regressed out using a Lagrange-multiplier method. The beam polarization, an important scaling factor, was measured to great accuracy with a set of Møller and Compton polarimeters. The CREX measurement set a world record in polarimetry precision.

The two experiments used the same basic setup, but there are some key differences between PREX-2 and CREX as highlighted in Table 1.

Table 1. Comparison between PREX-2 and CREX.

Feature	PREX-2	CREX
Target sample	Diamond- ^{208}Pb -Diamond	^{48}Ca
Target thickness	Diamond (90mg/cm ²) and ^{208}Pb (625mg/cm ²)	1 gm/cm ²
Beam energy	953 MeV	2.18 GeV
Beam current	70 uA	150 uA
Helicity flip rate	120 or 240 Hz	120 Hz
Helicity flip pattern	+ - - + or + - - + - + + - and complement	+ - - + and complement
Total charge collected	114 C	412 C
Main detector scattered flux	2.2 GHz per arm	26 MHz per arm
Mean kinematics	$0.00616 \pm 0.00005 \text{ GeV}^2$	$0.0297 \pm 0.0002 \text{ GeV}^2$

Both PREX-2 and CREX achieved remarkable suppression of systematic uncertainties as demonstrated by Table 2. After applying the necessary corrections and unblinding, the final measured asymmetries for PREX-2 and CREX were, respectively

$$A_{\text{PV}}^{208} = 550 \pm 16 \text{ [statistical]} \pm 8 \text{ [systematic]} \text{ ppb}, \quad (6a)$$

$$A_{\text{PV}}^{48} = 2668 \pm 106 \text{ [statistical]} \pm 40 \text{ [systematic]} \text{ ppb}. \quad (6b)$$

The combined PREX data provided the first meaningful constraint on the average interior baryon density of ^{208}Pb [1]:

$$\rho_0^b \approx 0.1480 \pm 0.0036 \text{ [experimental]} \pm 0.0013 \text{ [theoretical]} \text{ fm}^{-3}. \quad (7)$$

Accurate knowledge of ρ_0^b is critical for constraining ρ_0 and the isovector nuclear interactions that explain the structure of exotic neutron-rich nuclei [5]. Finally, the combined PREX and CREX experiments provided precise constraints on the neutron skins of ^{208}Pb and ^{48}Ca considering both experimental and model uncertainty

$$R_{\text{skin}}^{208} = 0.283 \pm 0.071 \text{ fm}, \quad (8a)$$

$$R_{\text{skin}}^{48} = 0.121 \pm 0.035 \text{ fm}. \quad (8b)$$

Table 2. Top 3 corrections and associated uncertainties for PREX-2/CREX [1, 2].

Correction	PREX-2	PREX-2	CREX	CREX
	Absolute [ppb]	Relative [%]	Absolute [ppb]	Relative [%]
Beam polarization	56.8 ± 5.2	10.3 ± 1.0	382 ± 13	14.3 ± 0.5
Beam trajectory and energy	-60.4 ± 3.0	11.0 ± 0.5	68 ± 7	2.5 ± 0.3
Beam charge	20.7 ± 0.2	3.8 ± 0.0	112 ± 1	4.2 ± 0.0
Total systematic uncertainty	± 8.2	± 1.5	± 40	± 1.5
Statistical uncertainty	± 16	± 2.9	± 106	± 4.0

3. Constraints on neutron-star radii

The combined PREX and CREX results have raised important questions regarding the understanding of nuclear structure and properties of neutron stars. There are interesting tensions between the results of these experiments and constraints from other methods.

Authors of [6] made predictions for several observable quantities using 16 different covariant energy density functionals. The models were calibrated to associate with a wide range of values of density dependence of symmetry energy (L) and the neutron skin of ^{208}Pb (R_{skin}^{208}). Using the strong correlation between the model predictions of the above quantities and the combined PREX result for R_{skin}^{208} , Ref. [6] constrained the slope of symmetry energy at two different densities

$$L|_{\rho_0} = 106 \pm 37 \text{ MeV}, \quad (9a)$$

$$L|_{\frac{2}{3}\rho_0} = 71.5 \pm 22.6 \text{ MeV}, \quad (9b)$$

where $\rho_0 \sim 0.15 \text{ fm}^{-3}$ is the nuclear saturation density. The central value of L obtained in this manner is at least 1 standard deviation away from constraints obtained via previous chiral EFT and *ab initio* calculations, strong probe measurements of neutron skins, nuclear electric dipole polarizability measurements, and quantum Monte Carlo calculations [6]. Consequently, the combined PREX result indicates a relatively high value for the pressure of neutron matter near ρ_0 , where the pressure is closely related to L . In other words, the combined PREX result supports a stiff equation of state near ρ_0 , where the pressure increases by a lot for a given increase in density. If this result is extrapolated to 1.4 solar mass neutron stars which typically have central densities of $2\text{--}3\rho_0$, the stiff equation of state would indicate a relatively large neutron star radius.

Further consequences are apparent from the combined constraints on the neutron skin of ^{208}Pb (R_{skin}^{208}), the radius value of a 1.4 solar mass neutron star ($R_*^{1.4}$), and neutron-star tidal deformability ($\Lambda_*^{1.4}$) based on the analysis by [6] as shown in figure 4:

$$0.21 \lesssim R_{\text{skin}}^{208} \text{ (fm)} \lesssim 0.31, \quad (10a)$$

$$13.25 \lesssim R_*^{1.4} \text{ (km)} \lesssim 14.26, \quad (10b)$$

$$642 \lesssim \Lambda_*^{1.4} \lesssim 955. \quad (10c)$$

The above constraint on tidal deformability is in 1 sigma tension with the LIGO GW170817 gravitational wave measurement which predicts $\Lambda_*^{1.4} \lesssim 580$ [9]. The LIGO measurement is more compliant with a smaller neutron-star radius than the lower limit set by PREX and a soft equation of state at the densities found in neutron stars.

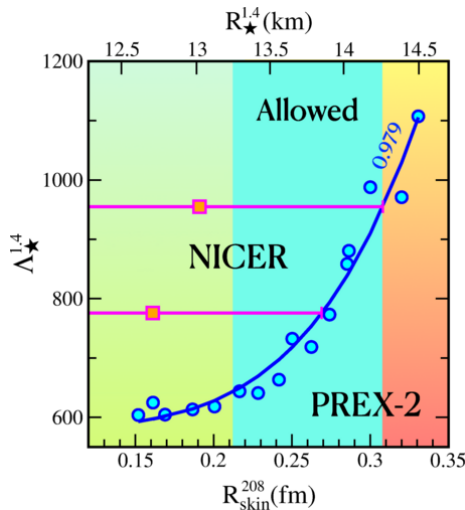


Fig. 4. (Colour on-line) The blue circles demonstrate neutron-star tidal deformability ($\Lambda_*^{1.4}$) predictions as a function of the neutron skin of ^{208}Pb (R_{skin}^{208}) and radius of a 1.4 solar mass neutron star ($R_*^{1.4}$) for a set of density functionals whose predictions for the later two quantities demonstrate a heavy linear correlation. The pink square points are constraints on the radius of the neutron star PSR J0030+0451 from the NICER telescope observations. The blue shaded region (middle) contains models that simultaneously satisfy the NICER constraints on $R_*^{1.4}$ and the PREX constraint on R_{skin}^{208} . The figure is reused with kind permission from the American Physical Society [6].

The CREX measurement of ^{48}Ca measurement adds another interesting dimension to this tension. The neutron skin predicted by ^{48}Ca is thinner than expectation if we hold the PREX result as a benchmark. In fact, a combined constraint on the PREX and CREX neutron skin measurements show approximately 2 standard deviation tension with the nearest DFT models and coupled cluster predictions [2] as shown in figure 5. The tensions between laboratory neutron-skin measurements [2, 6] and neutron-star gravitational wave observations [9] may indicate the equation of state assuming different stiffness at different densities. Such a scenario if validated would be indicative of exotic phase transitions in neutron-star interiors [3]. The PREX/CREX analysis introduces some model uncertainty when deducing R_{skin} from measured asymmetry using a 2-parameter Fermi function representing the weak charge density. Authors of Ref. [10] performed an alternate analysis without such a model dependence and still found it significantly challenging to simultaneously interpret PREX and CREX A_{PV} data with the current state-of-the-art nuclear EDFs. Reference [10] also demonstrated 1-sigma tension of PREX and CREX predictions with α_{D} measurements. The tensions can only be reconciled with further theoretical analysis and future experiments.

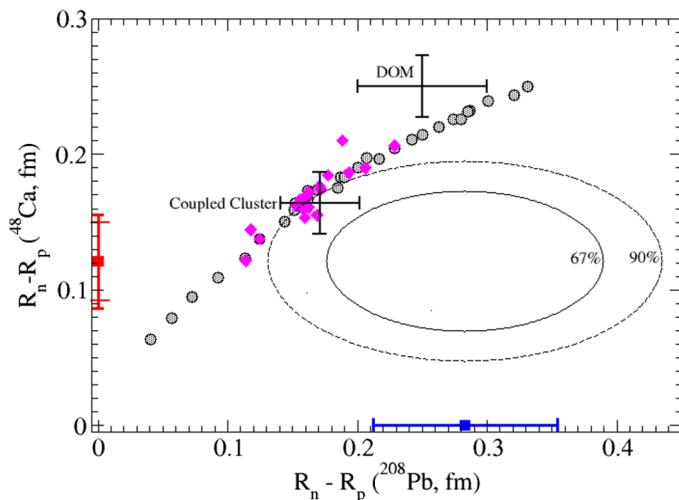


Fig. 5. (Colour on-line) Linear relationship between the ^{48}Ca neutron-skin *versus* ^{208}Pb neutron-skin predictions using relativistic (gray circles) and non-relativistic (magenta diamonds) density functionals. The figure also shows the coupled cluster and dispersive optical model predictions along with the combined confidence intervals from PREX and CREX. The figure is reused with kind permission from the American Physical Society [2].

4. Conclusion and future work

The combined PREX and CREX experimental results have shed new insight as well as raised questions regarding the structure of neutron-rich nuclei and neutron stars. PREX provided the first significant constraint on the interior baryon density of ^{208}Pb nucleus that closely approximates the nuclear saturation density (ρ_0) [1]. This is a path to constraining the isovector channel of nuclear effective interactions [5].

Combined analyses of the PREX/CREX data revealed tensions between the two measurements as well as tension with other methods [6, 10]. The PREX result is consistent with nuclear DFT models that predict a relatively high central value of nuclear symmetry pressure near ρ_0 and a relatively thick neutron skin for ^{208}Pb . On the other hand, the CREX result is consistent with models that predict a relatively low value of nuclear symmetry pressure at sub- ρ_0 densities and a relatively thin neutron skin for ^{48}Ca . Extrapolating the PREX prediction of stiff symmetry pressure for nuclei to neutron stars which have core densities of $2\text{--}3\rho_0$ would necessitate a relatively large radius for 1.4 solar mass neutron stars. This creates 1σ tension with the measurements of tidal deformability from the GW170817 gravitational wave event recorded by LIGO [9]. Tensions were also observed with nuclear electric dipole polarizability measurements (α_D) [10].

A two-parameter Fermi function was used in the primary analyses of PREX/CREX [1, 2]. One of the two parameters can be identified as a surface thickness. The associated uncertainty contributes to a model error for CREX which can be reduced by performing a separate measurement at different kinematics [5]. Another aspect of consideration is the heightened sensitivity of ^{48}Ca to the spin-orbit interactions compared to ^{40}Ca and ^{208}Pb [11]. In addition, the uncertainty on the PREX measurement is still too large for it to impose a meaningful constraint on the isovector sector of nuclear effective interactions [10]. Future measurements of these neutron skins by the Mainz Radius Experiment (MREX) will hopefully resolve the above issues. Additionally, further measurements of neutron star radii by the NICER telescope and better gravitational wave measurements from the LIGO–VIRGO–KAGRA Collaboration will provide new neutron-star data to compare against [3].

In addition to providing strong physics motivation, the improved systematic control of helicity-correlated beam asymmetries and several other PREX/CREX experimental innovations will inform the design of similar future experiments.

PREX-2 and CREX were supported by the U.S. Department of Energy, Office of Science, Office of Nuclear Physics Contract No. DE-AC05-06OR23177. The experiments also received additional support from the National Science Foundation and NSERC (Canada). I would also like to acknowledge the support from Jefferson Lab support staff for their assistance in conducting the experiments successfully. I would also like to extend special thanks to nuclear theorists who helped to interpret the results including C. Horowitz, B.T. Reed, J. Piekarewicz, P.G. Reinhard, X. Roca-Maza, J. Erler, and M. Gorchtein.

REFERENCES

- [1] PREX Collaboration (D. Adhikari *et al.*), *Phys. Rev. Lett.* **126**, 172502 (2021).
- [2] CREX Collaboration (D. Adhikari *et al.*), *Phys. Rev. Lett.* **129**, 042501 (2022).
- [3] J. Piekarewicz, F.J. Fattoyev, *Phys. Today* **72**, 30 (2019).
- [4] S. Rahman, «Using parity-violating weak interaction to measure neutron matter density and search for new physics», <https://www.osti.gov/biblio/>
- [5] B.T. Reed, Z. Jaffe, C.J. Horowitz, C. Sfienti, *Phys. Rev. C* **102**, 064308 (2020).
- [6] B.T. Reed, F.J. Fattoyev, C.J. Horowitz, J. Piekarewicz, *Phys. Rev. Lett.* **126**, 172503 (2021).
- [7] C.H. Rode, *AIP Conf. Proc.* **1218**, 26 (2010).
- [8] C. Gal, in: «Proceedings of 2020 Fall Meeting of the APS Division of Nuclear Physics», *American Physical Society*, 2020.
- [9] LIGO and Virgo collaborations (B.P. Abbott *et al.*), *Phys. Rev. Lett.* **121**, 161101 (2018).
- [10] P.-G. Reinhard, X. Roca-Maza, W. Nazarewicz, *Phys. Rev. Lett.* **129**, 232501 (2022).
- [11] C.J. Horowitz, J. Piekarewicz, *Phys. Rev. C* **86**, 045503 (2012).